Biomedical Optics EXPRESS

Novel catheter enabling simultaneous radiofrequency ablation and optical coherence reflectometry

D. Herranz,[1,*] Juan Lloret,[1] Santiago Jiménez-Valero,[1,2] J. L. Rubio-Guivernau,[1] and Eduardo Margallo-Balbás[1]

[1]*Medlumics S.L, Ronda de Poniente 6, 2A-B, 28760 Tres Cantos, Spain*
[2]*Servicio de Cardiología Intervencionista, Hospital Universitario La Paz, Madrid, Spain*
[*]*dherranz@medlumics.com*

Abstract: A novel radiofrequency ablation catheter has been developed with integrated custom designed optics, enabling real-time monitoring of radiofrequency ablation procedures through polarization-sensitive optical coherence reflectometry. The optics allow for proper tissue illumination through a view-port machined in the catheter tip, thus providing lesion depth control over the RF ablation treatment. The system was verified in an in-vitro model of swine myocardium. Optical performance and thermal stability was confirmed after more than 25 procedures, without any damage to the optical assembly induced by thermal stress or material degradation. The use of this catheter in RF ablation treatments may make possible to assess lesion depth during therapy, thus translating into a reduction of potential complications on the procedure.

OCIS codes: (110.4500) Optical coherence tomography; (120.4570) Optical design of instruments; (170.1020) Ablation of tissue; (170.3890) Medical optics instrumentation.

References and links

1. A. J. Camm, P. Kirchhof, G. Y. Lip, U. Schotten, I. Savelieva, S. Ernst, I. C. Van Gelder, N. Al-Attar, G. Hindricks, B. Prendergast, H. Heidbuchel, O. Alfieri, A. Angelini, D. Atar, P. Colonna, R. De Caterina, J. De Sutter, A. Goette, B. Gorenek, M. Heldal, S. H. Hohloser, P. Kolh, J. Y. Le Heuzey, P. Ponikowski, F. H. Rutten, "Guidelines for the management of atrial fibrillation: the Task Force for the Management of Atrial Fibrillation of the European Society of Cardiology (ESC)," Eur. Heart J. **31**(19), 2369–2429 (2010).
2. A. D´Silva and M. Wright, "Advances in Imaging for Atrial Fibrillation Ablation," Radiol. Res. Pract. 2011, 714864 (2011).
3. J. J. Langberg, H. Calkins, R. El-Atassi, M, Borganelli, A, Leon, S. J. Kalbfleisch and F. Morady, "Temperature monitoring during radiofrequency catheter ablation of accessory pathways," Circulation **86**, 5 (1992).
4. F. E. Marchlinski, D. J. Callans, C. D. Gottlieb, E. Zado, "Linear ablation lesions for control of unmappable ventricular tachycardia in patients with ischemic and nonischemic cardiomyopathy," Circulation **101**, 1288–1296 (2000).
5. P. C. Nardella, "Radio frequency energy and impedance feedback," Proc. SPIE **1068** (1989).
6. F. Perna, E. Kevin Heist, S. B. Danik, C. D. Barrett, J. N. Ruskin, M. Mansour, "Assessment of catheter tip contact force resulting in cardiac perforation in swine atria using force sensing technology," Circ. Arrhythm Electrophysiol **4**, 218–224 (2011).
7. A. Ames and W. G. Stevenson, "Catheter Ablation of Atrial Fibrillation," Cardiology Patient Page (2006).
8. L. S. Klein, H. Shih, F. K. Hackett, D. P. Zipes, and W. M. Miles, "Radiofrequency catheter ablation of ventricular tachycardia in patients without structural heart disease," Circulation **85**, 1666–1674 (1992).
9. M. A. Wood, "Exposing gaps in linear radiofrequency lesions: form before function," Circ. Arrhythm Electrophysiol **4**, 257–259 (2011).

#236397 Received 22 Apr 2015; revised 2 Jul 2015; accepted 21 Jul 2015; published 7 Aug 2015

10. H. Wang, W. Kang, T. Carrigan, A. Bishop, N. Rosenthal, M. Arruda and A. M. Rollins, "In vivo intracardiac optical coherence tomography imaging through percutaneous access: toward image-guided radio-frequency ablation," J. Biomed. Opt. **16**(11), (2011).
11. M. Wright, E. Harks, S. Deladi, F. Suijver, M. Barley, A. van Dusschoten, S. Fokkenrood, F. Zuo, F. Sacher, M. Hocini, M. Haïssaguerre and P. Jaïs, "Real-time lesion assessment using a novel combined ultrasound and radiofrequency ablation catheter," Heart Rhythm **8**, 304–312 (2011).
12. D. C. Adler, C. Zhou, T. H. Tsai, H. C. Lee, L. Becker, J. M. Schmitt, Q. Huang, J. G. Fujimoto and H. Mashimo, "Three-dimensional optical coherence tomography of Barrett´s esophagus and buried glands beneath neo-squamous epithelium following radiofrequency ablation," Endoscopy **41**(9), 773–776 (2010).
13. X. Fu, Z. Wang, H. Wang, Y. T. Wang, M. W. Jenkins and A. M. Rollins, "Fiber-optic catheter-based polarization-sensitive OCT for radio-frequency ablation monitoring," Opt. Lett. **39**, 17 (2014).
14. C. K. Hitzenberger, E. Götzinger, M. Sticker, M. Pircher and A. F. Fercher, "Measurement and imaging of birefringence and optic axis orientation by phase resolved polarization sensitive optical coherence tomography," Opt. Express **9**, 13 (2001).
15. J. M. Guerra, E. Jorge, S. Raga, C. Gálvez-Montón, C. Alonso-Martín, E. Rodríguez-Font, J. Cinca and X. Vinolas, "Effects of open-irrigated radiofrequency ablation catheter design on lesion formation and complications: in vitro comparison of 6 different devices," J. Cardiovasc Electrophysiol **24**(10), 1157–62 (2013).
16. H. Nakagawa, F. H.M. Wittkampf, W. S. Yamanashi, J. V. Pitha, S. Imai, B. Campbell, M. Arruda, R. Lazzara, W. M. Jackman, "Inverse relationship between electrode size and lesion size during radiofrequency ablation with active electrode cooling," Circulation **98**, 458–465 (1998).
17. A. Oron, N. Reshef, Y. Beer, T. Brosh and G. Agar, "The influence of radiofrequency ablation patterns on length, histological and mechanical properties of tendons," Muscles, Ligaments and Tendons Journal **2**(2), 85–90 (2012).
18. S. Foppen, "Experimental and numerical analysis of lesion growth during cardiac radiofrequency ablation," BMTE (2009).

1. Introduction

Radiofrequency ablation (RFA) is currently a well-established treatment for cardiac arrhythmias [1, 2]. To date, the effectiveness of lesion formation during RFA is evaluated by indirect measures- like catheter tip temperature [3], electrograms amplitude [4], impedance [5] or monitoring catheter-tissue contact force [6]. However, there are no clinically available methods that allow for direct assessment of lesion formation during RF energy delivery.

Atrial fibrillation (AF) is the most common arrhythmia in clinical practice [7]. RFA is an effective treatment in patients with paroxysmal AF [8]. However its adoption is hampered by a relatively high incidence of AF recurrence after an initially successful procedure. RFA for AF needs to generate deep and extensive lesions, creating "lines" of necrotic tissue in the left atrium wall to electrically isolate the pulmonary veins. Recurrence of AF may be related with incomplete RFA lesions, due to lack of transmurality or continuity of the ablation lines [9]. In addition, uncontrolled RFA in the thin wall of the atrium may cause dangerous complications, like cardiac perforation. Understanding lesion science allows delivery of optimal therapy. So, the possibility of direct imaging of tissue during RFA might be useful to establish the efficacy of lesion formation and, thus, to improve clinical outcome reducing the risk of complications over the procedure.

Recently, some reports have revealed the potential utility of optical [10] and ultrasound imaging [11] technologies in RFA applications. Both techniques are able to identify RF lesions and allow for the differentiation between ablated and non-ablated tissue, detecting early signs of overtreatment, and, thus helping to prevent complications. Optical coherence tomography (OCT) may have some advantage for a good control over RF ablation procedure due to the higher axial resolution. Polarization-sensitive OCT (PS-OCT) has also demonstrated its ability to detect changes in the birefringence properties of atrial tissue after RFA applications. Until now, the experiments have been done using separate RF catheter and PS-OCT probe [12, 13]. In these works, simultaneous optical imaging of the tissue region where RF energy is delivered has been a challenge. This may have been due to the need for mechanical beam scanners, which are even more complex to implement in a real clinical setting, where the catheter design should

#236397 Received 22 Apr 2015; revised 2 Jul 2015; accepted 21 Jul 2015; published 7 Aug 2015

be simple to manufacture, easy to use and robust.

The development of an integrated catheter that combines polarization-sensitive optical coherence reflectometry (PS-OCR) and RF capabilities, allowing real-time evaluation of lesion depth is reported for the first time. We demonstrate the validity of the optical design, being compatible with the irrigation channels and having no-interference with the RF energy delivered. We observe substantial changes over the accumulated phase retardation due to birefringence properties of tissue, which were lost after ablation procedure. High accuracy over the tip and tissue contact was observed.

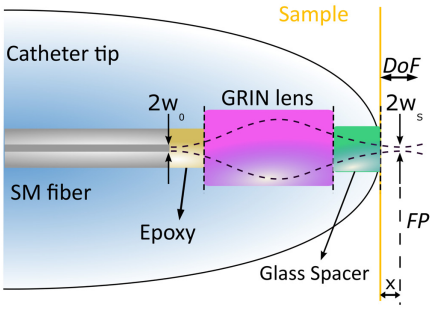

Fig. 1. Sketch-based modeling used for the focal length calculations.

2. Catheter design

A customized 7-Fr-diameter steerable RF ablation catheter (Vascomed GmbH) has been used as a basis for the development of the device. The catheter has a tip electrode equipped with a temperature sensor. To record electrical activity from within the heart, 3 ring electrodes have been implemented. The catheter has also been designed with the corresponding electrical wiring and mechanical features enabling RF energy delivery from the generator and controllable deflection. A 500-μm-diameter through hole is machined in the tip, thus implementing an optical view-port.

The custom optics are comprised by a single-mode (SM) optical fiber followed by an off-the-shelf gradient index (GRIN) rod lens from GRINTech GmbH (model GT-LFRL-050-028-50-AF). The lens diameter is 0.5 mm and both sides of the GRIN lens are 8° angled cut to reduce back-reflections. The distance (x) between the spacer and the focal plane (FP) was required to be a half of the depth of field (DoF) (see Fig. 1). As it is defined by Eq. (1), the beam waist radius (w_s) in the focal plane is fully determined by the DoF and the center wavelength (λ). The DoF is related to the A-scan depth, being for this particular case 1.5 mm in air and λ is 1.32 μm.

$$w_s = \sqrt{\frac{DoF \times \lambda}{2\pi}} = 17.752\mu m \tag{1}$$

Taking into account that the mode field radius (w_0) of the light propagating through the SM optical fiber is 4.45 μm, measured at $1/e^2$ (OFS AllWaveFlex), the magnification factor (m) of the optical system is:

$$m = \frac{w_s}{w_0} = 3.989 \tag{2}$$

To meet the requirements on the DoF and x simultaneously, a second degree of freedom is needed. In particular, a glass spacer implemented by N-BK7 material with similar refractive

#236397 Received 22 Apr 2015; revised 2 Jul 2015; accepted 21 Jul 2015; published 7 Aug 2015

index is assembled to the GRIN lens, which fixes a null working distance (*WD*) by properly designing its length. The optical design has been optimized using a ray tracing software (ZEMAX v.13). The design parameter is the GRIN lens length. Figure 2(a) shows the ZEMAX results after optimizing both design lengths by a custom metric function. Finally, the GRIN lens and the glass spacer lengths are set to be 1.31 mm and 1.24 mm, respectively. Microscope images showing details of the fabricated custom optics can be seen in Figure 2(b) and 2(c). The optics is inserted in a cylindrical glass ferrule resulting in enhanced mechanical robustness and it is assembled by gluing using UV-curable epoxy.

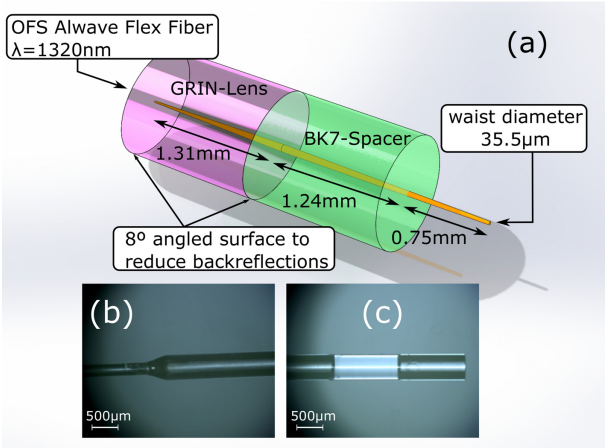

Fig. 2. (a) Optical simulations using Zemax. (b) and (c) depict the optical assembly by optical microscope featuring 5x magnification (optical fiber with corresponding ferrule, GRIN lens and glass spacer).

In order to study the catheter implementation on the RFA therapy, the optical losses (*L*) have been measured when the catheter is mechanically straight and while operating in maximum deflection configuration, because the optics should has losses compatible with high-quality and high-speed imaging. Deflection refers to movement of the catheter tip independent of the rest of the catheter. The minimum radius of curvature (*ROC*) and the *L* increase when the catheter is deflected to its maximum value. During in-vivo procedures, deflections of at least 180° are required. This movement has been controlled by a mechanical actuator placed in the proximal part. The optical losses in logarithmic units have been represented by:

$$L = -10log_{10}\left(\frac{P}{P_{ref}}\right) \tag{3}$$

Where the reference power (P_{ref}) at the light source output is collected by using a large-area Ge-doped free-space power meter (Thorlabs PM100D). Following, the optical power at the catheter output (*P*) is also collected by the same detector. For this measurements, the space in-between the catheter and the active area of the power meter is about 2 mm, thus guaranteeing the exposure of the total light leaving the catheter or the optical connector. The typical result for 5 different catheters is shown in Table 1, which have accepted optical losses for PS-OCR images of biological tissues when the catheter is deflected to its maximum value, verifying the feasibility of the catheter design.

#236397 Received 22 Apr 2015; revised 2 Jul 2015; accepted 21 Jul 2015; published 7 Aug 2015

Table 1. Typical L value for 5 different integrated catheter. The L has been measured as a function of the deflection angle (θ). The table represents when the catheter is maximally deflected (i.e. minimum radius of curvature (ROC) and maximum optical losses (L)) and when it is straightened.

ROC (mm)	$L_{\theta=180^\circ}$ (dB)	$L_{\theta=0^\circ}$ (dB)	ΔL (dB)
46	0.45	0.36	0.09

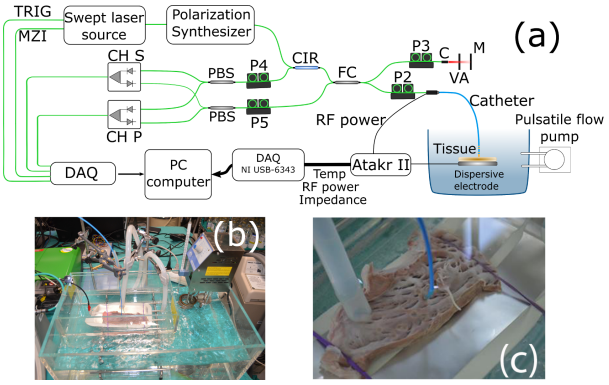

Fig. 3. (a) Sketch of the experimental setup. The system consists of a swept laser source (SS), polarizer (P), polarized beam splitter (PBS), fiber coupler (FC), circulator (CIR), collimator (C), variable attenuator (VA) and mirror (M). (b) and (c) show a picture of the in-vitro chamber. and catheter contact with the cardiac swine tissue, respectively.

3. Experimental setup

The experimental setup depicted in Fig. 3 comprises a polarization-sensitive swept source OCT system and a RF power generator. The OCT system is based on the OCS1300SS (Thorlabs Inc.) with a frequency swept laser centered at 1300 nm, which is able to penetrate multi-layer biological tissues with a 11.7 μm of axial resolution measured. From the laser source, two orthogonal polarization states of the interference fringe signals are detected using a fiber polarization beam splitter. The biological tissue birefringence induces phase-retardation between polarization states of light, which can be recovered from the detected interference signals [14], acquired at full-speed of the swept laser source (8 kAscan/s). The typical optical power collected at the catheter output is 1 ± 0.1 mW with around 97 dB of SNR. RF energy was applied between the catheter tip electrode and an indifferent lead placed below the tissue by an Atakr II (Medtronic) in unipolar mode. A continuous unmodulated sinusoidal signal oscillating at 484.2 kHz was delivered in power-control mode in the 20-40W range or temperature-control limited to 80°C during 30-60s.

A standard experimental in-vitro setup has been used [15]. Left ventricular and atrial strips form a freshly excised swine heart were mounted on a platform and placed in a chamber filled with saline solution maintained at 37°C (Fig. 3(b)). The temperature was controlled with an immersion thermostat (Termotronic II, JP Selecta). As shown in Fig. 3(c), the catheter was mounted in a holder maintaining perpendicular contact with the endocardial surface of the tissue to enhance the RFA effectiveness on the lesion formation [16]. A pulsatile saline flow of 2 l/min generated by a peristaltic pump (Watson-Marlow 520SN) was directed to the point of contact between ablation electrode and tissue through a plastic tube placed at a distance of 2 cm from the ablation electrode.

#236397 Received 22 Apr 2015; revised 2 Jul 2015; accepted 21 Jul 2015; published 7 Aug 2015

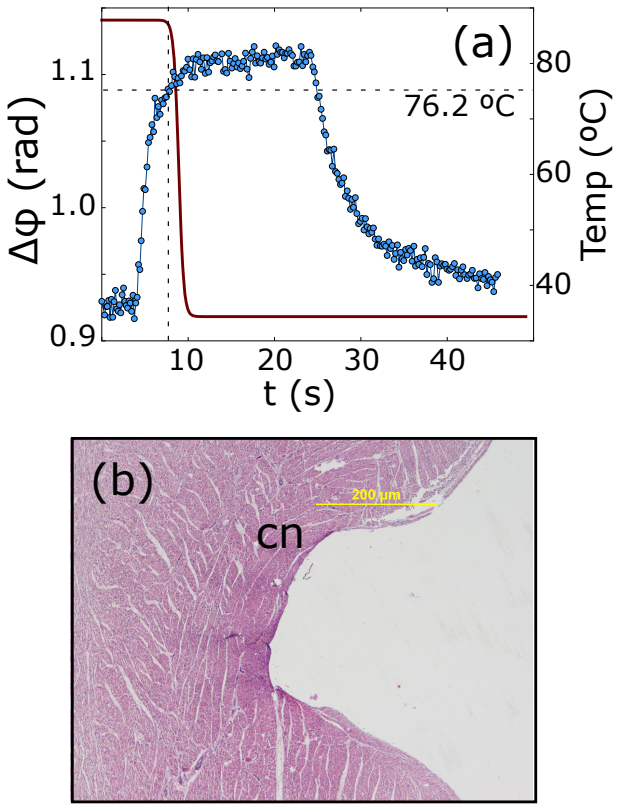

Fig. 4. (a) Accumulated phase retardation and temperature evolution in time of an in-vitro swine myocardium at tissue surface. (b) A characteristic histology sample collected from ablated tissue, where complete or partial loss of membrane borders is shown. Coagulative necrosis has been denoted by cn.

4. Experimental results

The birefringence of the tissue fibers may be altered due to a number of potential factors outside of the ablation procedure. It is known that connective biological fibers such as collagen exhibit birefringent properties. When full tissue necrosis is attained by heat transfer, oriented collagen degrades. This denaturation produces a loss of the birefringent behavior of these fibers. Irreversible denaturation of collagen fibers occurs at about 70°C [17]. Cell death is caused by a combination of an applied supraphysiological temperature and duration. However, a partial loss of birefringence may be indicative of partial tissue damage (edema), which may ultimately compromise the efficacy of the procedure. We have carried out an in-vitro experiment demonstrating the feasibility of real-time optical monitoring of RF ablation of myocardial tissue using an integrated catheter. The experiments were done in saline solution, however in presence of blood PS-OCR imaging is also feasible and allows the evaluation of tip-tissue contact [13]. A phase retardance on the tissue surface respect to time has been represented in Fig. 4(a). As it is expected, the birefringence tissue properties close to the tip disappear after reach temperature higher than 70°C [17]. To evaluate the treatment after the ablation, sections of myocardial tissue were obtained around each lesion, fixed in formaline and stained with hematoxylin-eosin for histological analysis. Fig. 4(b) represents typical histological study revealing observable microscopic alteration.

#236397 Received 22 Apr 2015; revised 2 Jul 2015; accepted 21 Jul 2015; published 7 Aug 2015

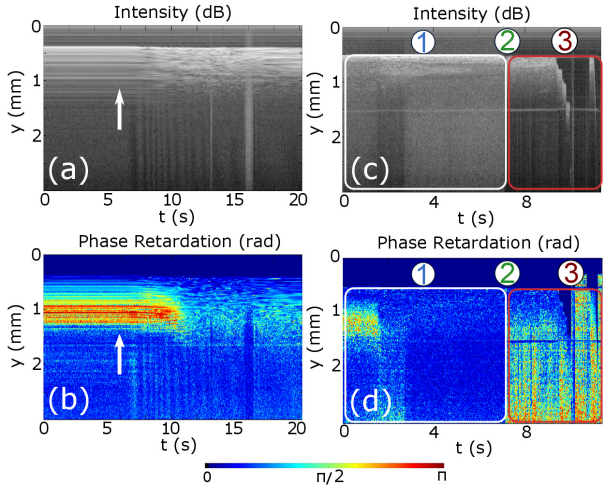

Fig. 5. Representative OCR images of an in-vitro swine myocardium with the forward imaging catheter probe: (a) and (b) show the structural and accumulated phase retardation evolution in time (M-scan), respectively. The measurement was done applying 40W and the arrow represents the time instant when the RF power start to be applied. (c) and (d) show the recorded structural and polarization sensitive signal for RFA treatment when the tip moves, respectively. Region 1 represents the RFA time interval, in 2 slippage appears and in 3 the contact is lost.

Figures 5(a) and 5(b) show, respectively, the structural and phase delay of a M-scan during the RFA procedure. Power-control mode has been used at 40W during 45s, reaching a maximum tip temperature of 60°C. The untreated myocardium exhibits a significant phase retardance, while the tissue birefringence properties disappear after applying enough RF power. The combination of structural and polarization-sensitive images gives additional information, which is not possible to derive when using one of the techniques alone. Structural measurement is more sensitive to refractive index changes, having more contrast in the first tissue layers, while the phase delay is accumulated and depends on the birefringence of tissue, obtaining more information about the lesion depth. This is to our knowledge the first successful RFA treatment with real-time monitoring supported by PS-OCR and implemented in a single integrated catheter.

One of the possible problems during the procedure in real patients is the contact lost between catheter tip and tissue due to catheter displacement. In Fig. 5(c) and 5(d) is represented an experiment in which after some period of time, the tip moves along the myocardium surface and the perpendicular alignment was lost. During the experiment three regions are well defined. In region 1, normal RFA procedure is happening, similar to previous treatment, but after 7s a slippage occurs (denoted with 2), losing the good contact in the time interval in 3. This measurement reveals the ability of PS-OCR to evaluate RF catheter-tissue contact.

Time lesion formation measured in terms of the time to lose birefringence (10-90%) as a function of total time (i.e. since RF energy is applied until the birefringence is lost) is shown in Figure 6. The lesion formation always heads uphill, leading towards a steady state after a time. An explanation for this is related to dissipated heat (Q_{diss}) [18], which in a biological tissue is defined by $Q_{diss} = Q_{heat} + Q_{cond} + Q_{conv}$. Where no contribution of external heat sources is taken into account. In our system, Q_{heat} represent the energy needed to elevate the system temperature, Q_{cond} is related to the energy conducted through the tissue and Q_{conv} is the convection

#236397 Received 22 Apr 2015; revised 2 Jul 2015; accepted 21 Jul 2015; published 7 Aug 2015

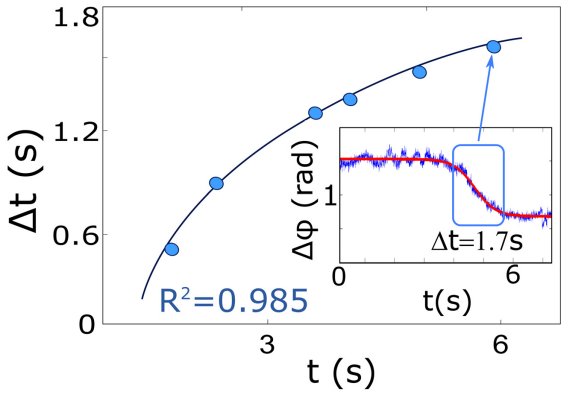

Fig. 6. Figure represents the time dependence of the ablation process at 1 mm below the surface. The insets show the criteria for analyze the time dependence.

by flowing the saline solution. Part of the thermal energy is absorbed by the swine myocardium and fluid, being lost as tissue overheats. As a consequence, at low power the effective time required for the lesion formation is higher than when the power increases, reaching a steady state at maximum tissue power absorption.

5. Conclusion

We have presented a novel catheter design with an optical access for real-time tissue probing in radiofrequency ablation applications. We have demonstrated the absence of interference between optical coherence reflectometry signals and the delivery of radiofrequency energy. Phase retardation in polarization sensitive M-scans showed strong contrast between ablated and untreated tissue, probably due to the thermal denaturation of oriented collagen present in the extracellular matrix of myocardial tissue. This endogenous molecular marker of tissue condition would provide rich insight into the thermal dynamics of the ablation process, potentially enabling real-time in-vivo monitoring of lesion depth. This design may open the door for optically guided RF ablation therapy, improving treatment control and thus, opening a new path to better clinical results. Better understanding of lesion science should be evaluated by optical response regarding the creation of necrosis “lines” in tissue by microscopic images. Next steps also include extending the current catheter to have direct imaging in multiple directions so as to cover the full active volume around the RF electrode to support in-vivo procedures.

Acknowledgments

The authors acknowledge Rafael Peinado MD, PhD for his interest and support.

#236397 Received 22 Apr 2015; revised 2 Jul 2015; accepted 21 Jul 2015; published 7 Aug 2015